Structural modulation in the orbitally induced Peierls state of $MgTi_2O_4$

2008 J. Phys.: Condens. Matter 20 275230

(http://iopscience.iop.org/0953-8984/20/27/275230)

J. Phys.: Condens. Matter **20** (2008) 275230 (5pp) doi:10.1088/0953-8984/20/27/275230

Structural modulation in the orbitally induced Peierls state of $MgTi_2O_4$

H X Yang[1], B P Zhu[2], L J Zeng[1], H F Tian[1], C Ma[1], J Shi[2] and J Q Li[1,3]

[1] Beijing National Laboratory for Condensed Matter Physics, Institute of Physics, Chinese Academy of Sciences, Beijing 100080, People's Republic of China
[2] Department of Physics, Wuhan University, Wuhan 430072, People's Republic of China

E-mail: ljq@aphy.iphy.ac.cn

Received 12 March 2008, in final form 17 May 2008
Published 6 June 2008
Online at stacks.iop.org/JPhysCM/20/275230

Abstract

The structural properties associated with the orbitally induced Peierls transition in $MgTi_2O_4$ are characterized by *in situ* cooling TEM observations. A distinctive structural modulation with the wavevector of $\mathbf{q}_1 = 1/4\ (0, 0, 4)$ has been well demonstrated below a critical temperature of about 260 K for $MgTi_2O_4$. Systematic analysis demonstrates that this structural modulation can be well explained by an orbital order existing in the low-temperature insulating phase. It is also noted that the nonstoichiometric feature commonly appearing in the present system could yield visible changes in both physical and structural properties. A low-temperature study of the microstructure of $Mg[Ti_{1.9}Mg_{0.1}]O_4$ reveals that a little substitution of Mg^{2+} for Ti^{3+} ions on the octahedral sites can disrupt the long-range order of the t_{2g} orbitals, resulting in complex tweed structures in the superstructure phase.

The spinel oxides AB_2O_4 are a remarkable family of numerous compounds with significant physical properties, such as superconductivity [1], heavy fermion phenomena [2], charge ordering [3] and unusual magnetic properties [3, 4]. Recently, $MgTi_2O_4$ has attracted considerable interest due to notable physical and structural properties correlated with a low-temperature metal–insulator (M–I) transition. This compound has a cubic spinel structure at room temperature and undergoes a phase transition to a tetragonal structure at about 260 K [5]. Schmidt *et al* pointed out that the low-temperature structure of $MgTi_2O_4$ contains ordered Ti–Ti dimers in an unusual helical pattern [6]; Khomskii suggests that this dimerization pattern in association with an orbital ordering transition could open a modest gap in the low-temperature insulator and this kind of phase transition can be thought of as an orbitally induced Peierls transition in three-dimensional systems [7]. Although certain fundamental structural features of $MgTi_2O_4$ have been investigated by synchrotron and neutron powder diffraction [6], the microstructural properties and local structural distortion related to the low-temperature M–I transition have not been examined in the earlier literature. In this paper, we will report on the *in situ* TEM observations of $MgTi_2O_4$ and $Mg[Ti_{1.9}Mg_{0.1}]O_4$ from room temperature down to 20 K. The experimental results demonstrate that the low-temperature helical dimerization pattern of $MgTi_2O_4$ can be well characterized by a structural modulation with wavevector $\mathbf{q}_1 = 1/4(0, 0, 4)$. It is also noted that the samples with slightly nonstoichiometric composition, such as $Mg[Ti_{1.9}Mg_{0.1}]O_4$, show notable tweed-patterned domains as small as a few nanometers.

Polycrystalline samples of $MgTi_{2-x}Mg_xO_4$ material were synthesized using a spark plasma sintering method as described in a previous paper [8]. Structural and compositional analysis suggests that a small amount of Mg^{2+} often occupies the Ti^{3+} sites and produces the nonstoichiometric $MgTi_{2-x}Mg_xO_4$ compounds. This nonstoichiometric feature could yield visible changes in both physical and structural properties in the present system, as discussed in the following context. Specimens for transmission electron microscopy (TEM) observations were polished mechanically with a Gatan polisher to a thickness of around 50 μm and then ion-milled by a Gatan-691 PIPS ion miller. A TECNAI 20 operating at a voltage of 200 kV, equipped with low-temperature sample stages, was used for the microstructural investigation from room temperature down to 20 K. The magnetic susceptibility and resistivity measurements were performed with a Quantum Design Measurement System (PPMS).

[3] Author to whom any correspondence should be addressed.

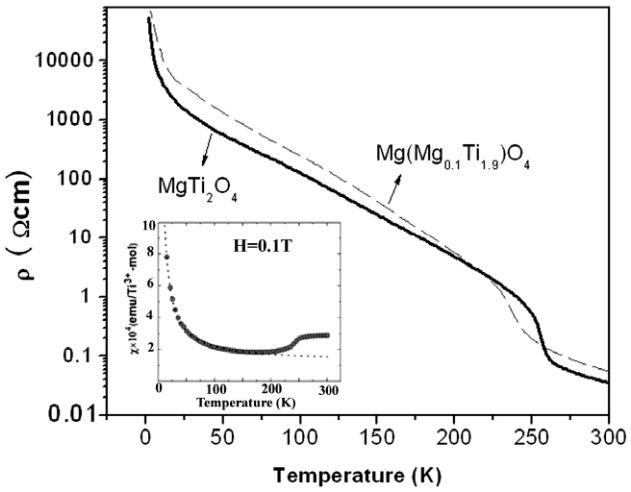

Figure 1. Temperature dependence of resistivity for $MgTi_2O_4$ and $Mg[Ti_{1.9}Mg_{0.1}]O_4$ demonstrating notable anomalies at about 260 K in both samples. The inset shows the temperature dependence of magnetic susceptibility for $MgTi_2O_4$.

Two high-quality samples with slightly different chemical compositions have been carefully investigated in the present study. Sample A has the lattice parameter of $a = 8.5081$ Å with a stoichiometric composition as compared with the reported data [6, 9]. Sample B is a nonstoichiometric sample of $Mg[Ti_{2-x}Mg_x]O_4$ with a lattice parameter of $a = 8.5030$ Å. According to the earlier literature, the lattice parameter for the $Mg[Ti_{2-x}Mg_x]O_4$ materials changes systematically with the chemical composition following roughly Végard's law [9], which allows the estimation of x in the nonstoichiometric $Mg(Ti_{2-x}Mg_x)O_4$ samples by a formula of $x = 1 - [a - 8.4409]/0.0691$. Hence, the sample B used in the present study has the composition of $Mg[Ti_{1.9}Mg_{0.1}]O_4$ based on the experimental x-ray diffraction data.

The M–I transition in this kind of material often yields remarkable anomalies in both physical and structural properties. Figure 1 shows the experimental results of the temperature dependence of resistivity and magnetic susceptibility (inset) obtained from an $MgTi_2O_4$ polycrystalline sample. A sharp upturn in resistivity and an abnormal drop in magnetic susceptibility can be easily recognized in association with the phase transitions at around 260 K [5, 8, 9]. These remarkable changes are attributed to an orbitally induced Peierls transition accompanied by the creation of a spin singlet on a Ti–Ti dimer in the low-temperature insulating state [5, 7–9]. The resistivity obtained from $Mg[Ti_{1.9}Mg_{0.1}]O_4$ is also shown in figure 1 for comparison; it is noted that the slightly nonstoichiometric feature can broaden the phase transition and shifts T_c to a lower temperature in comparison with that of $MgTi_2O_4$.

The stoichiometric $MgTi_2O_4$ material has a typical cubic spinel structure at room temperature (RT) [6]. Figures 2(a)–(c) show, respectively, the electron diffraction patterns taken along the [100], [110] and [111] zone axis directions at about 300 K. All main diffraction spots in these patterns can be well indexed by a cubic cell with a lattice parameter of $a = 8.5081$ Å and a space group of $Fd\bar{3}m$; these results are consistent with the neutron and x-ray data as reported in previous publications [6, 9].

In order to understand the structural evolution that occurs along with this M–I phase transition, we have performed careful *in situ* cooling TEM observations on both sample A and sample B from room temperature down to 20 K. Figures 2(d)–(f) show the relevant electron diffraction patterns taken at about 100 K for $MgTi_2O_4$. The remarkable feature revealed in our low-temperature (LT) observations is the presence of the clear additional weak superstructure spots following each fundamental spot in the LT patterns. Detailed electron diffraction examination demonstrates that all these superlattice spots became clearly visible only at temperatures below 260 K. This fact suggests that a notable structural transition accompanying this M–I transition occurs in the present system. Though these superlattice spots are very weak in some areas, they are, in general, very sharp corresponding to a coherence length longer than 50 nm (see figures 2(d)–(f)).

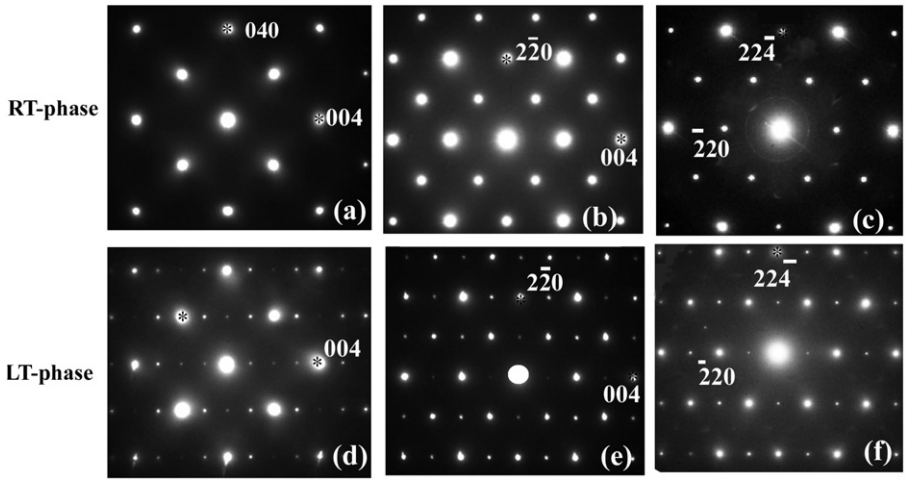

Figure 2. Electron diffraction patterns of $MgTi_2O_4$. (a)–(c) show the selected-area diffraction patterns taken along the [100], [110] and [111] zone axis directions at room temperature, respectively. (d)–(f) show the selected-area diffraction patterns taken along the [100], [110] and [111] zone axis directions at 100 K, respectively, clearly revealing additional spots along the ⟨001⟩ and ⟨110⟩ directions in the LT phase. The indexes in these patterns are based on cubic notation.

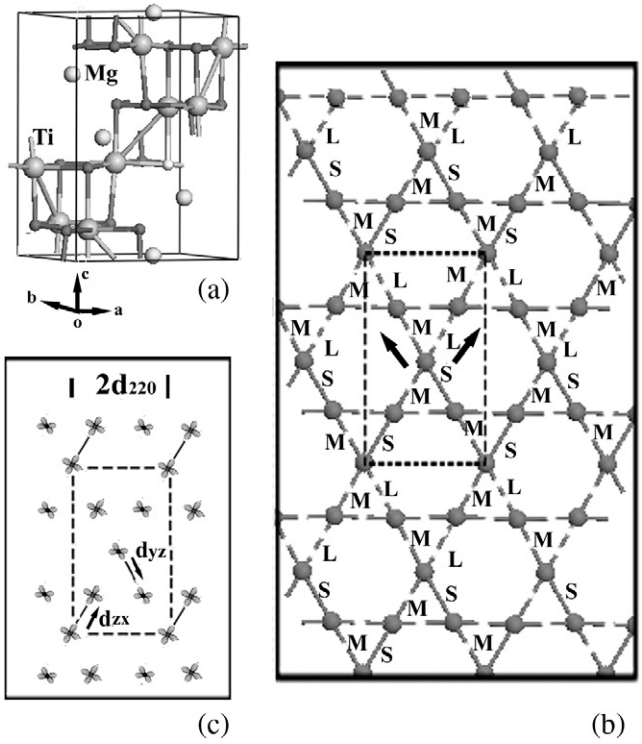

Figure 3. Schematic structural models for an LT $MgTi_2O_4$ structure. (a) A primitive tetragonal unit cell of $a_c/\sqrt{2} \times a_c/\sqrt{2} \times a_c$. (b) Structural model projected along the [111] zone axis direction of the cubic cell, demonstrating a single layer of Kagome plane with ordered arrangement of short (S), intermediate (M) and long (L) bonds along two different chains. (c) The d_{yz} and d_{zx} orbital chains in one supercell; only the shortest bonds were illustrated.

The wavevector of the superstructure in figures 2(d)–(f) can be written as $q_1 = (004)/4$ and $q_2 = (220)/2$. As a matter of fact, the $(220)/2$ modulation can be reduced to $(004)/4$ by adding an allowed reciprocal lattice vector of $(1, 1, -1)$, i.e. $q_2 = q_1 + (11\bar{1})$. Hence, all diffraction patterns of figures 2(d)–(f) reveal the presence of this same modulation in different cross sections of the reciprocal lattice. In agreement with the measurements of x-ray and neutron powder diffractions, our careful analysis suggests that this LT modulated structure can be fundamentally described by a primitive tetragonal unit cell of $a_c/\sqrt{2} \times a_c/\sqrt{2} \times a_c$ with a non-centrosymmetric space group of $P4_12_12$ or $P4_32_12$ [6]. Figure 3(a) shows a structural model of an LT primitive tetragonal unit cell [6], which shares the same c axis with respect to the room temperature cubic spinel lattice while the a and b axes are rotated by 45°.

Considering the complex LT structural features in the present system, the structural transition in $MgTi_2O_4$ has been extensively discussed in the earlier literature using two different approaches. The first one illustrates the LT phase by an unusual chirality in which short (S) and long (L) bonds form 'S–L–S–L helices' running along the c axis [6]; on the other hand, from the orbital ordering point of view, the transition-metal Ti in the $MgTi_2O_4$ structure is located in regular O_6 octahedra, and the dominant crystal field therefore splits the d levels into the t_{2g} triplet and e_g doublet. For a Ti^{3+} ion, only t_{2g} levels are occupied by one electron [10] with an equal probability distributed, respectively, on the d_{xy}, d_{yz} and d_{zx} orbitals. Since each orbital has its specific shape and orientation, d_{xy}, d_{yz} and d_{zx} orbitals in spinels are found to be oriented along the typical chains formed by the Ti ions [7, 10]. The lattice symmetry of $MgTi_2O_4$ is lowered in the LT insulator to a tetragonal structure [6]. According to the calculated band structure [6, 7], this tetragonal distortion increases the bandwidths of the d_{zx} and d_{yz} bands, and decreases that of d_{xy}. The electron on Ti^{3+} occupies the lowest doubly degenerate d_{zx} and d_{yz} level, and the d_{xy} band located above the Fermi level is unoccupied. In this case, the d_{yz} (or d_{zx}) orbital in a Ti chain is quarterly occupied. This configuration could result in the Peierls instability and lead to the tetramerization [7, 9–12]: an ordered arrangement of short, intermediate, long and intermediate bonds along the d_{yz} and d_{zx} chains, with the spin-singlet states at the short bonds. This ordered state is recognizable as a superstructure, being visible along the four crystallographically equivalent ⟨110⟩ directions.

Figure 3(b) shows a schematic structural model for a (111) plane in the spinel $MgTi_2O_4$ structure, illustrating the orbital ordered tetramerization state within a Kagome lattice layer of Ti atoms. This view emphasizes that any two of the three intersecting edge-sharing TiO_6 chains at a Ti site defines a plane with a Kagome topology of Ti sites. A third chain would extend out of the figure at each site. The Mg sites lie at points directly above and directly below the centers of the hexagonal holes in the Kagome lattice [11]. Concerning the orbital ordering tetramerization state mentioned above, two sets of ordered arrangements of short, intermediate and long bonds are clearly indicated in two Ti chains (four crystallographically equivalent ⟨110⟩ directions), respectively. The basic unit for the orbital order in a single Kagome topologic layer is shown by the dashed line. This ordered state projected along the [111] zone axis direction could give rise to a face-centered superstructure of $2d_{220} \times 4d_{224}$ as shown in figure 2(f). Figure 3(c) shows schematically the d_{yz} and d_{zx} orbital order in one supercell, in which the occupied orbitals and the shortest bond are clearly illustrated.

In order to compare our experimental data with previous structural results obtained from x-ray diffraction, we have carried out a theoretical calculation based on the orbital ordering model as shown in figure 3. According to our calculations, the longer bond of Ti–Ti is 3.13 Å and the shortest one is 2.88 Å. These data are based on the results of neutron diffraction [6] and slightly adjusted by comparing our experimental results with the calculated ones. Figures 4(a) and (b) show the theoretical diffraction patterns along the [111] and [100] zone axes, respectively, and both are in good agreement with the experimental patterns in both reflection conditions and spot intensities of the superstructure.

The better and clearer views of the superstructure with a visible tetramerization pattern corresponding to an alternation of short, intermediate, long and intermediate bonds [7] can be obtained along the [100] zone axis direction. Figure 5(a) shows a schematic structural model for the LT superstructure projected along the [100] zone axis direction, in which the shortest Ti–Ti bonds and the orbital ordering wave are schematically illustrated. Figure 5(b) shows a [001] zone axis

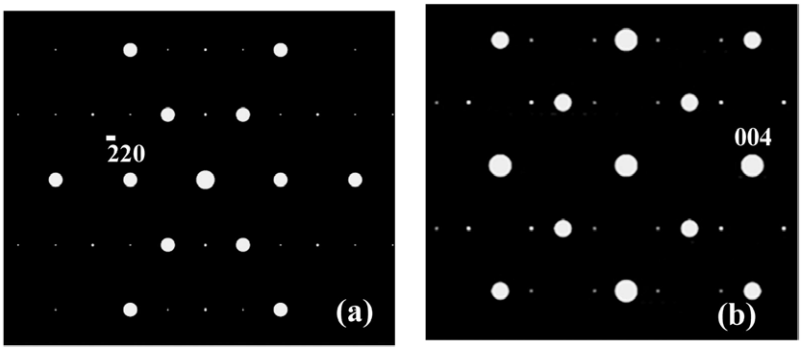

Figure 4. Theoretical diffraction patterns for LT $MgTi_2O_4$ along (a) [111] and (b) [100] zone axis directions showing the satellite spots corresponding to the orbital ordering modulation.

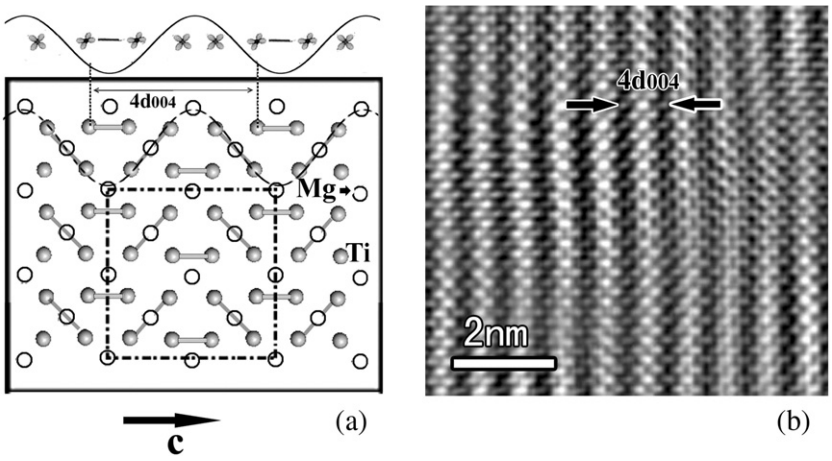

Figure 5. A schematic structural model for the LT phase projected along [100] zone axis directions, with only the shortest Ti–Ti bond labeled for clarity, demonstrating a wavevector $q = 1/4(0, 0, 4)$ caused by atomic displacement and bond type modulations. A schematic view of a t_{2g} orbital density wave is presented at the top. The dashed line is the cubic cell. (d) [100] zone axis high-resolution electron microscopy (HREM) image for $MgTi_2O_4$ taken at a temperature of 100 K.

high-resolution TEM image for an $MgTi_2O_4$ crystal taken at a temperature of 100 K. This micrograph was obtained from a thin region of the crystal; therefore, the modulation with a periodicity of $4d_{004}$ waves can be clearly recognizable along the *c*-axis direction. The regular array of dark fringes can directly correspond to the orbital ordering pattern within a picture of tetramerization.

It is also noted that the electron diffraction patterns obtained from certain areas in an $MgTi_2O_4$ crystal often show the doublet superstructure modulations, as typically illustrated in figure 6(a). This kind of multi-set modulation actually comes from areas containing twinning domains of the superstructures. We further cooled the sample to 20 K, and no evident structural change was observed in the temperature range from 100 K down to 20 K.

Structural investigations on the nonstoichiometric Mg $[Ti_{2-x}Mg_x]O_4$ materials demonstrated that a small deviation of chemical composition from the stoichiometric $MgTi_2O_4$ phase evidently affects the M–I phase transition (see figure 1) and low-temperature structural features. Figures 6(b)–(d) show a number of electron diffraction patterns and a high-resolution TEM image for $Mg[Ti_{1.9}Mg_{0.1}]O_4$ taken at about 100 K. It is remarkable that the additional superstructure spots in the insulating phase show up as diffused spots, directly suggesting a much shorter coherent length (<10 nm) than that in the $MgTi_2O_4$. Electron diffraction observations along the main zone axis directions often reveal doublet or triplet weak spots from different twinning variants. Typical examples are shown in figures 6(b) and (c). Figure 6(d) shows a high-resolution TEM image of the $Mg[Ti_{1.9}Mg_{0.1}]O_4$ taken along the [100] direction at about 100 K, illustrating complex nanodomains with clear structural modulation along the [001] direction with a periodicity of $4d_{004}$. The image directly demonstrates the short-range order state for the tetramerization pattern in the nonstoichiometric sample of $Mg[Ti_{1.9}Mg_{0.1}]O_4$. Di Matteo *et al* [12, 13] considered the tendency to form this particular orbital ordering configuration rather than all other possibilities by calculating the energy of a collection of tetrahedra with different bonding configurations, and found that a set of one-dimensional decoupled Heisenberg chains had a higher energy per site than a collection of isolated 'B-type' tetrahedra. This conclusion suggests that an increase of x in the $Mg[Ti_{2-x}Mg_x]O_4$ system will introduce Mg^{2+} on the octahedral Ti^{3+} sites, which could disrupt the well-defined long-range orbital order along a specific chain. Therefore, complex nanodomains with visible structural modulations

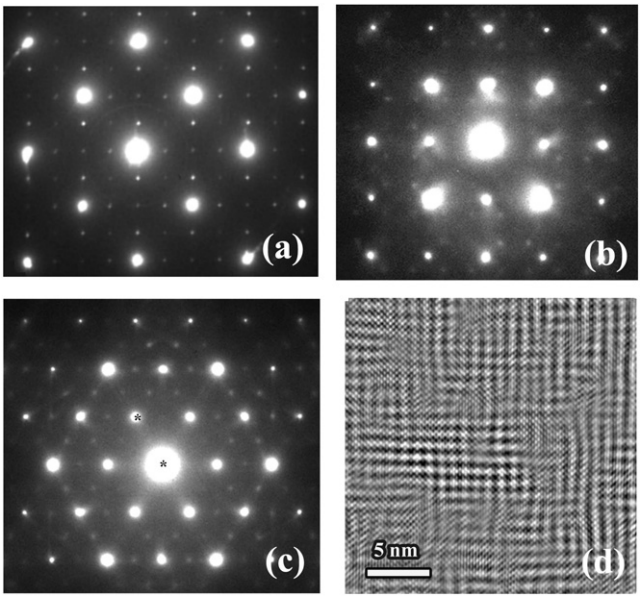

Figure 6. Electron diffraction pattern taken from an area covering twin domains in $MgTi_2O_4$ at 100 K. Electron diffraction patterns taken at 100 K along (b) [100] zone axis direction and (c) [111] zone axis direction of LT-phase $Mg[Ti_{1.9}Mg_{0.1}]O_4$, exhibiting the diffused superstructure spots of twinned patterns. (d) HRTEM image taken along the [001] zone axis direction at 100 K, demonstrating complex nanodomains with modulated structures.

appear in the low-temperature insulating phase. The decrease of the critical temperature in $Mg[Ti_{1.9}Mg_{0.1}]O_4$ may arise from certain alterations of electronic structures due to a small amount of Mg^{2+} substituted for Ti^{3+} in this spinel system.

In summary, we have systematically investigated the structural features of $MgTi_2O_4$ by *in situ* cooling TEM observations from 300 K down to 20 K. A distinctive structural modulation, $\mathbf{q}_1 = 1/4(0, 0, 4)$, has been observed in the low-temperature insulated phase of $MgTi_2O_4$. Systematic analysis demonstrates that the structural modulation can be well explained by the previously reported orbital ordered state through the classical Peierls transition. It is also noted that partial substitution of Ti by Mg ions results in complex nanodomains of superstructures due to disruption of long-range order of Ti orbits along specific chains.

Acknowledgments

We would like to thank Y Li for her help during TEM sample preparation. We are grateful to Professor N L Wang for help during the manuscript preparation. This work is supported by the National Science Foundation of China, the Knowledge Innovation Project of the Chinese Academy of Sciences, and the 973 projects of the Ministry of Science and Technology of China.

References

[1] Johnston D C, Prakash H, Zachariasen W H and Viswanathan R 1973 *Mater. Res. Bull.* **8** 777
[2] Kondo S, Johnston D C, Swenson C A, Borsa F, Mahajan A V, Miller L L, Gu T, Kojima A I, Luke G M, Uemura Y J, Chmaissem O and Jorgensen J D 1997 *Phys. Rev. Lett.* **78** 3729
[3] Fujiwara N, Yasuoka H and Ueda Y 1998 *Phys. Rev.* B **57** 3539
[4] Urano C, Nohara M, Kondo S, Sakai F, Takagi H, Shiraki T and Okubo T 2000 *Phys. Rev. Lett.* **85** 1052
[5] Isobe M and Ueda Y 2002 *J. Phys. Soc. Japan* **71** 1848
[6] Schmidt M, Ratcliff W II, Radaelli P G, Refson K, Harrison N M and Cheong S W 2004 *Phys. Rev. Lett.* **92** 056402
[7] Khomskii D I and Mizokawa T 2005 *Phys. Rev. Lett.* **94** 156402
[8] Zhu B P, Tang Z, Zhao L H, Wang L L, Li C Z, Yin D, Yu Z X, Tang W F, Xiong R, Shi J and Ruan X F 2007 *Mater. Lett.* **61** 578
[9] Zhou H D and Goodenough J B 2005 *Phys. Rev.* B **72** 045118
[10] Zhou J, Wang N L, Li G, Luo J L, Ma Y C, Wu Dan, Zhu B P, Tang Z and Shi J 2006 *Phys. Rev.* B **74** 245102
[11] Croft M, Kiryukhin V, Horibe Y and Cheong S W 2007 *New J. Phys.* **9** 86
[12] Radaelli P G 2005 *New J. Phys.* **7** 53
[13] Di Matteo S, Jackeli G, Lacroix C and Perkins N B 2004 *Phys. Rev. Lett.* **93** 077208